ELSEVIER

Sedimentary Geology 125 (1999) 47–59

Sedimentary Geology

Combining a computer simulation and eustatic events to date seismic sequence boundaries: a case study of the Neogene of the Bahamas

Animikh Sen *, Christopher G.St.C. Kendall, Philip Levine

Department of Geological Sciences, University of South Carolina, Columbia, SC 29208, USA

Received 25 November 1997; accepted 2 November 1998

Abstract

This paper demonstrates that the principles of seismic sequence stratigraphy and the techniques of computer simulation can be combined to date the sedimentary section. As an example it uses the Neogene section of the western shelf of the Straits of Andros in the Bahamas. To this end, type I, second-order seismic sequence boundaries were identified on a seismic cross-section from the region. These were used as brackets to correlate enclosed third-order events with an eustatic sea-level curve. The interpreted section was then reproduced using a computer simulation program. The simulation successfully reproduced the onlapping geometries of the shelf margin identified on the seismic section. The early Neogene fill of the Straits of Andros is assumed to have had an uncomplicated and uniform tectonic setting. This simplified the inputs to the simulation, which focused on capturing the sedimentary response to the eustatic changes. Inputs included a constant rate of subsidence of 0.009 m/ka, a uniform linearly increasing rate of carbonate accumulation from 28.5 Ma to 11.5 Ma, and the sea-level cycle chart of Haq et al. (1987), updated for the Neogene with the absolute ages provided by Berggren et al. (1995). The subsequent graphical output shows a good match to the interpreted seismic. This suggests that the amplitude and ages of the sea-level changes as shown in the eustatic chart can be used to date the sequence boundaries for the Neogene of the Straits of Andros. It also establishes that for areas of known subsidence, simulation techniques can be used to date seismic sections where biostratigraphic data are poor.

Keywords: sea level; sequence stratigraphy; computer simulation; Bahamas; Neogene

1. Introduction

Sequence stratigraphers interpreting seismic lines are confronted with the difficulty of determining: (a) the ages of sequence boundaries interpreted on the seismics (Miall, 1990); and (b) the size of eustatic sea-level changes associated with those (Burton et al., 1988). This paper suggests that computer simulations of seismic cross-sections can be used in conjunction with principles of sequence stratigraphy to solve these two problems. To this end a seismic cross-section, that records the Neogene carbonate fill of the Straits of Andros in Great Bahamas Bank, was interpreted, and a sedimentary simulation, SEDPAK (Moore, 1997) based on empirical modeling was used to reproduce the interpretation. At the heart of this study is the recognition that eustatic events are evidenced in sedimentary sections by the presence of synchronous sedimentary sequences and the unconformities that bound them (Vail et al., 1977). These eustatic events produce changes in the accommodation for sedimentary fill that have worldwide extent. Their chronostratigraphic correlation is dependent

* Corresponding author. Fax: +1-803-777-6610; E-mail: animikh@sc.edu

0037-0738/99/$ – see front matter
PII: S0037-0738(98)00147-X

upon reliable time markers spaced sufficiently close in time to bracket the sediment packages formed in response to changes in sea level. The measurement of the amplitudes of sea-level events on the sea-level charts are dependent on assumptions related to the rates of subsidence and sediment accumulation for the regions in which the charts were created (Burton et al., 1988). There appears to be no direct method available to measure these amplitudes of sea-level variation. This is because there is no datum available from which to measure, particularly since the earth surface constantly moves, (1) in response to sediment compaction, (2) isostatic response to sediment loads, and (3) thermal tectonic movement (Burton et al., 1988). The relative positions of sea level are thus dependent on tectonic behavior and eustatic position, and the size of either of these two variables can only be measured by assuming a model for the other's behavior. Methods used to measure sea level indirectly have to assume models of tectonic behavior. Such methods include tide gauges, strandline position (which assume a continental relief in addition to tectonic behavior), paleobathymetry, seismic sequence onlap, stacked subsidence curves, and the matching of sequence geometries with graphical simulations (Burton et al., 1988). Despite the fact that sea-level amplitudes cannot be measured independently stratigraphic predictions based on eustatic sea-level curves and/or tectonic models of behavior can be reproduced and verified away from areas of interest. This is because the onlapping or downlapping of sediment geometries are dependent on rates of sedimentation, tectonic movement and sea-level position. So if it is assumed that the sea-level fluctuations are the same at different locations, any change in accommodation will be the product of the local tectonics and sedimentation. However, in a particular area, if rates of subsidence and of carbonate accumulation are constant for several cycles in eustatic sea level, the frequency and amplitude of the onlapping sequence geometries will be the product of the frequency and amplitude of the changes in eustatic sea level. Our hypothesis is, if the sequence geometries of a sedimentary simulation generated with the eustatic sea level match those interpreted on seismic lines, then the ages of these latter sequences have the same timing as the former. The shallow-water carbonate platform of the Strait of Andros in the Bahamas provides a perfect opportunity to test this hypothesis.

2. Assumptions

To simulate stratigraphic interpretations which incorporate the size of sea-level events, geologic sections are required for which it can be assumed that there was a uniform rate of subsidence and a high rate of constant sediment accumulation, for several sea-level cycles. In these cases the resultant accommodation and its fill is sufficient to be recorded on seismic sections. Examples for such settings include the Neogene of the Bahamas Platform, the Lower Cretaceous of offshore South Africa (Brown et al., 1995), the onshore seismic record of the Lower Cretaceous of the NPRA (Bird and Molenaar, 1992; Ryan, 1997) and the cliffs of Neogene carbonate on the Island of Mallorca (Pomar, 1993). For all these areas, the changing onlapping position of the sequence geometries are assumed to have been produced through several cycles of sea-level change and to be independent of tectonics. In the absence of absolute sea-level markers for a paleoshore, it is assumed that the rate of sedimentation was sufficient to fill any shoreward accommodation to sea level. In this case the equivalent bedding plane and the shelf margin can then be used as a proxy of the sea-level position. This assumption is a reasonable one for a carbonate shelf (especially in areas of high sediment production and low tectonic subsidence) and the identification of confirmatory paleobathymetric markers (Eberli et al., 1997) proves its validity. The reasonableness of this assumption can be seen in the seismic sections of the Neogene of the Bahamas (Fig. 2) and the cliffs of Neogene sediments exposed in the cliffs of the Island of Mallorca (Pomar, 1993). The sedimentary sections developed at both these locations are the product of carbonate accumulation rates high enough to fill the accommodation space up to sea level during each sea-level cycle. In both cases, the Neogene section is expressed by prograding clinoforms enveloped shoreward by aggrading horizontal shelfal units. In the Bahamas, this effect can be seen at both the western side of the bank and in an interior sea, the Straits of Andros (Eberli and Ginsburg, 1989).

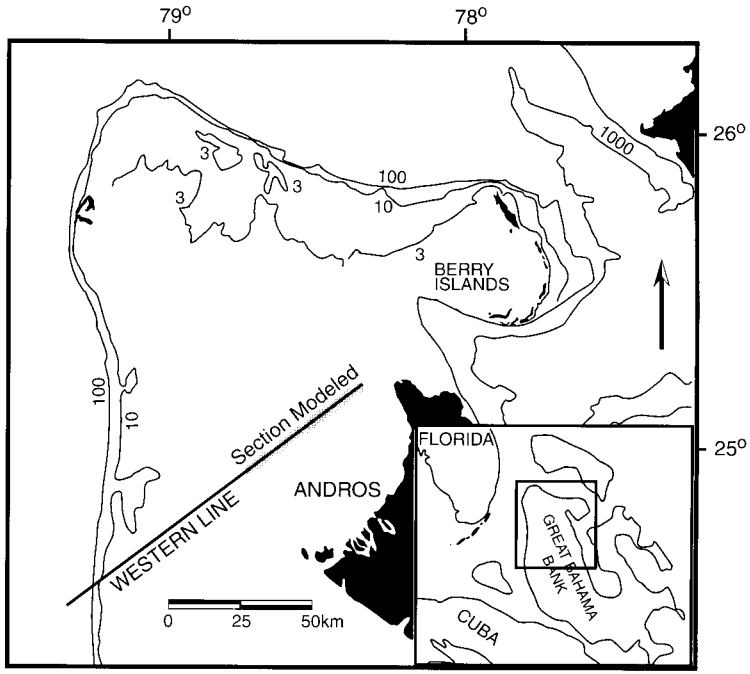

Fig. 1. Map of Great Bahamas Bank showing the Western line and the section of the line modeled in this paper. Four depth contours (1000, 100, 10 and 3 m) are shown.

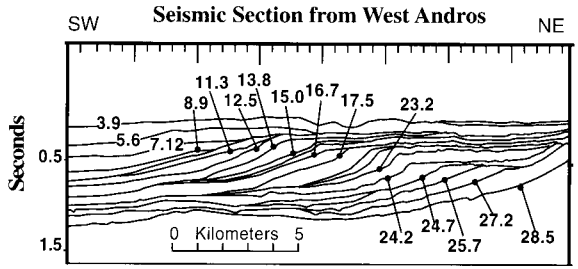

Fig. 2. Line drawing of the interpreted seismic section from the Andros Channel, Bahamas, showing the major sequence boundaries identified in the section with their interpreted ages.

3. Sequence stratigraphic analysis and simulation of the Straits of Andros

3.1. Introduction to the data set

The establishment of the sequence stratigraphy of the Straits of Andros involves an interpretation of the carbonate platform based on seismic data and the limited well control from the western Great Bahamas Bank (Fig. 1). This Bahamian seismic data set consists of a cross-bank profile (Fig. 2). The top 1.7 s (two-way travel time) were used for the study on the western side of Great Bahamas Bank. Seven wells have been drilled along this seismic line; one of them, ODP site 1007, reached the base of the Neogene. Seismic profiles of the northwestern Great Bahamas Bank have been interpreted to document the lateral growth potential of isolated platforms that were welded together by margin progradation to form larger banks (Eberli and Ginsburg, 1987, 1989). The mechanism responsible for the evolution of the carbonate margin from aggradation to progradation is thought to be sediment overproduction with respect to accommodation on the platform (Hine et al., 1981; Wilber et al., 1990). Excess sediment was transported offbank and decreased the accommodation space on the marginal slope. Progradation occurred in pulses that are interpreted to be the result of third-order sea-level fluctuations (Eberli and Ginsburg, 1989). The biologic and sedimentary data from the wells from the Bahamas transect have corroborated this (Eberli et al., 1997).

3.2. Methodology for updating the sea-level curve

Recent biostratigraphic studies suggest that some of the Neogene ages on the Haq et al. (1987), sea-level chart are inaccurate. For the purpose of this study we have updated the ages on the late Neogene portion of this chart. The ages of the nannofossils and magnetic polarity reversal boundaries of Berggren et al. (1995), were used to update and define the timing of 'sequence boundary ages' on the Haq et al. (1987) curve (Tables 1 and 2) which matched periods of maximum sea-level fall. To enable comparison with the sequence boundaries identified on ODP Leg 166 (which were given ages from the nannofossil zones), the ages derived from nannofossil horizons were given preference over those derived from polarity reversals. The updated 'sequence boundary ages' on the Haq et al. (1987) curve are shown in Table 3. The updated ages and the corresponding magnitudes of sea-level position from the Haq et al. (1987) curve were then used to draft a sea-level curve (Neogene Curve, NC). The intermediate ages of sea-level position between sequence boundaries were linearly interpreted. This Neogene Curve (NC) was then used as an input to the simulations described in this study.

Table 1
Comparison of nannofossil ages from the sea-level chart of Haq et al. (1987) and from the time scale of Berggren et al. (1995)

Nannofossil biochronozones (lower boundary)	Ages from Haq et al. (Ma)	Ages from Berggren et al. (Ma)
NN21	0.25	0.25
NN20	0.50	0.50
NN19	1.95	1.95
NN18	2.5	2.5
NN17	2.6	2.6
NN16	3.5	3.75
NN15	4.0	4.05
NN14	4.5	4.15
NN13	5.0	5.0
NN12	5.5	5.6
NN11	8.1	8.5
NN10	9.0	9.5
NN09	10.0	11.2
NN07	11.8	11.9
NN06	13.6	13.6
NN05	16.1	15.6
NN04	17.8	18.2
NN02	21	23.2
NNO1	25	24
NP25	28.6	27.6
NP24	30.5	29.9

Table 2
Comparison of the ages of magnetic polarity chronozones from the sea-level chart of Haq et al. (1987) and from the time scale of Berggren et al. (1995)

Chronozone	Ages from Haq et al. (Ma)	Ages from Berggren et al. (Ma)
C1	1.8	1.8
C2	2.6	2.6
C2A	4.0	4.15
C3	5.5	5.9
C3A	6.8	7.45
C4	7.9	8.7
C5	11.9	11.9
C5A	15	14.8
C5B	16.1	16
C5C	17.55	17.25
C5D	18.5	18.25
C5E	19.45	19.05
C6	20.9	20.5
C6A	22.8	22.55
C6B	23.9	23.35
C6C	25.5	24.7
C7	26.35	25.58
C7A	26.95	25.85
C8	28.2	27.05
C9	29.8	28.25
C10	31.5	29.4

3.3. Seismic stratigraphic interpretation

Eberli and Ginsburg (1989) previously correlated sequence boundaries on a seismic section across the Straits of Andros to 'sequence boundaries' on the Haq et al. (1987) chart. In this study this line was reinterpreted and correlated with the Neogene Curve (NC) with its new sequence boundary ages. Second-order type I unconformities were first identified on the seismic on the basis of their more extensive erosional character. Their correspondence with the 'sequence boundaries' associated with the second-order sea-level events on the Neogene Curve (NC) was noted. Using those as brackets, third-order type I unconformities were then identified on the seismic with their enclosed equivalent seismic sequences and correlated with the third-order 'sequence boundaries'

Table 3
Comparison of third-order seismic sequence boundary ages of the sea-level chart of Haq et al. (1987) and that of the Neogene Curve (NC), the later being updated from the time scale of Berggren et al. (1995)

Third-order cycles	Ages from Haq et al. (Ma)	NSILC (this paper) ages (Ma)
TB 3.10	0.8	0.75
TB 3.9	1.6	1.6
TB 3.8	2.4	2.4
TB 3.7	3.0	3.1
TB 3.6	3.8	3.91
TB 3.5	4.2	4.1
TB 3.4	5.5	5.6
TB 3.3	6.3	7.12
TB 3.2	8.2	8.92
TB 3.1	10.5	11.3
TB 2.6	12.5	12.5
TB 2.5	13.8	13.8
TB 2.4	15.5	15
TB 2.3	16.5	16.7
TB 2.2	17.5	17.7
TB 2.1	21	23.2
TB 1.5	22	24.2
TB 1.4	25.5	24.7
TB 1.3	26.5	25.7
TB 1.2	28.4	27.2
TB 1.1	30.0	28.5

on the Neogene Curve (NC). As can be seen from the interpretation of the seismic data, the major events on the Neogene curve (NC) have produced distinct stratigraphic signals (Fig. 2). For instance, following the large sea-level fall at 28.5 Ma, a major unconformity would have been expected and so the major erosional event on the seismic is interpreted to be equivalent to this. This unconformity separates the upper Neogene carbonate accumulation from the lower Tertiary and the Cretaceous. Similarly, a major fall in sea level at 11.3 Ma has also produced a corresponding major unconformity on the seismic section. It is apparent that the sea level fell below the shelf margin, with the resulting unconformity bracketing a series of third-order sea-level events which date between 28.5 Ma and 11.3 Ma. While examining the geometric position of these latter sequences with respect to the shelf margin, and counting them, it can be seen that more unconformities can be identified than there are events on the sea-level chart. Despite these additional sequences, there appears to be a good correspondence of the lateral extent and thickness of the different sequences on the seismic (Fig. 2) with the amplitude and duration of the different sea-level events (Fig. 3). Having made the sequence stratigraphic interpretation, a simulation of this interpretation was developed. The causes for these extra sequences are yet to be determined and their origin is the subject of further research. It is suspected that some of these extra sequences may be a result of inadvertent interpretation of the products of both low and high stand cycles of sea level as sequences. Other extra sequences may be the products of fourth-order sea-level events.

3.4. Simulation program and input parameters

The SEDPAK simulation software was used to simulate the sedimentary geometries in this study. SEDPAK was developed in University of South Carolina and is a forward modeling program. Information on this program can be found in a mathematical discussion by Kendall et al. (1989) and Strobel et al. (1989). A geometrical description of SEDPAK is given in Moore (1997).

3.5. Time interval

The last 28.5 Ma of platform evolution of the Great Bahamas Bank/Straits of Andros was modeled using 114 time steps of 250 ka duration. This number of time steps was considered essential for the proper resolution of the simulation so it captured the effects of all the sea-level events (Table 4).

3.6. Initial basin surface

The initial depositional surface of the Straits of Andros used in the simulation was derived from the seismic line. This is interpreted as a type I second-order sequence boundary with an age of 28.5

Table 4
Input parameter used during simulation of the Andros channel (see text for detail) — time interval

Time steps in simulation	
Duration	Number
250 ka	114

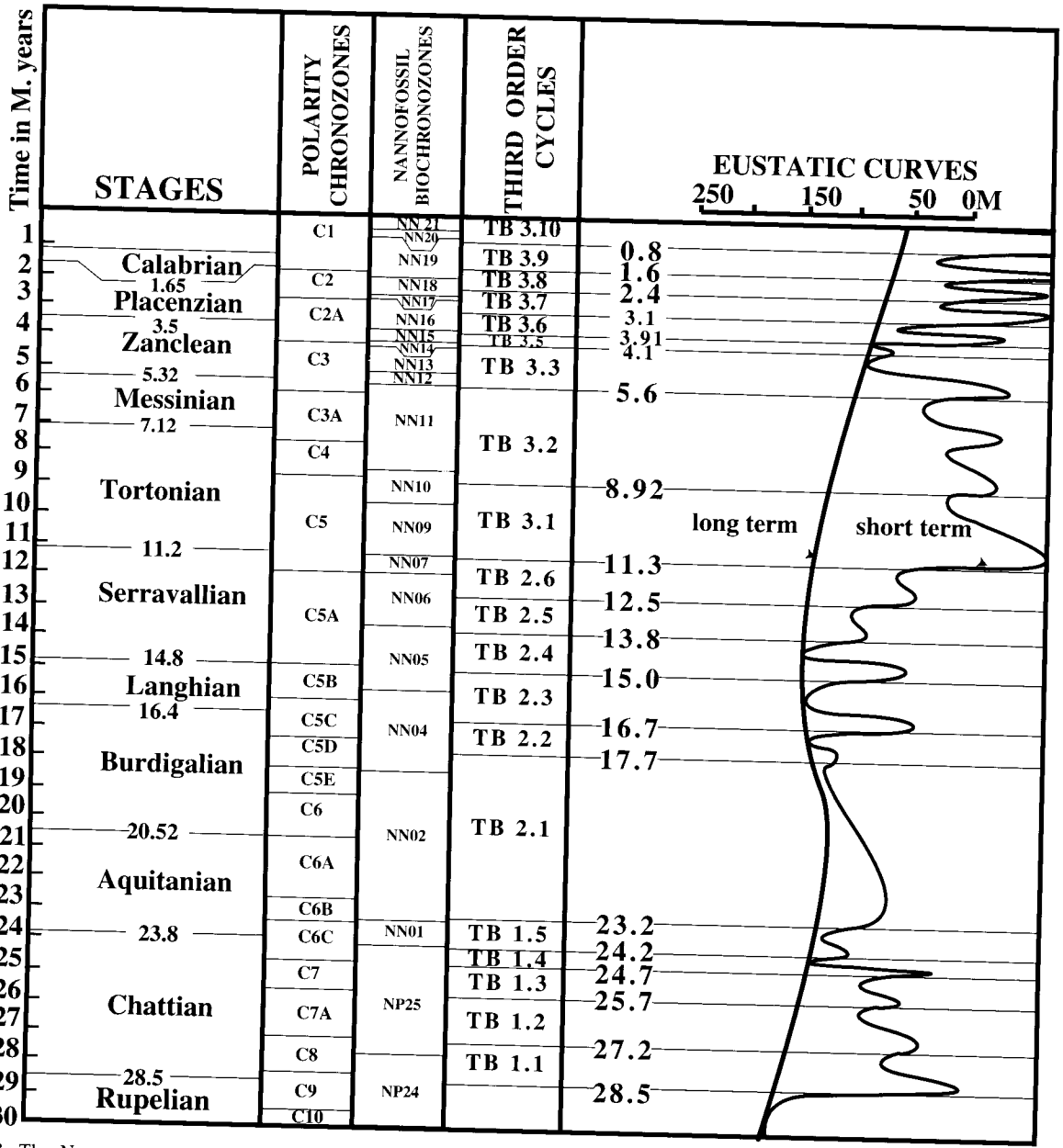

Fig. 3. The Neogene curve (NC) showing the polarity chronozones and nannofossil biochronozones and the third-order sequence boundaries with their updated ages. Based on Haq et al. (1987) and Berggren et al. (1995).

Ma (Fig. 2). The time–depth conversion of this surface and the other sequence boundaries above it were determined from the velocity profile of the Great Isaac well (Eberli and Ginsburg, 1989). The Straits of Andros is interpreted to have initially formed as an asymmetric trough approximately 30 km wide with a depth of approximately 370 m (Table 5). For the purposes of the simulation runs, the basin was divided into 60 columns, each with a width of 0.5 km.

Table 5
Input parameter used during simulation of the Andros channel (see text for detail) — initial basin surface

Distance (km)	Depth (m)
0	−370
18	−370
26	−71
28	21

3.7. Eustatic sea level

The sea-level curve that was used for the modeling is shown in Fig. 3 and is the Neogene Curve (NC) described earlier.

3.8. Tectonic movement

The subsidence history of the Great Bahamas Bank–Straits of Andros data set was derived directly from the seismic section and was initially modeled by simulating the basin with no sediment fill. The thickness of the sediment measured on the seismic crossing the platform was used as a first approximation in the determination of the changes in the rate of subsidence. In the simulation runs these rates were changed as a function of time and location across the basin, reflecting the low-frequency changes in accommodation space at different time intervals as well as different locations. A constant rate of 0.009 m/ka was used between 28.5 Ma and 11.3 Ma and faster rates were used thereafter in order to ensure that there would be enough space available to accommodate the shelfal and bank margin carbonates as they were generated (Table 6).

3.9. Carbonate deposition

Benthic carbonate production rates in the simulation mimic the response to photosynthesis of carbonate-producing organisms. Most of the Bahamian Bank carbonate sediments were produced by organisms that were dependent upon light, so production rates decreased rapidly with increasing water depth (Schlager, 1981). The simulation models sediment accumulation, thus including the cumulative effects of production and penecontemporaneous erosion. This

Table 6
Input parameter used during simulation of the Andros channel (see text for detail) — tectonic movement

Subsidence rates (m/ka) at specified locations as a function of time			
Time (Ma)	Location across the basin in km		
	1.0000	17.0000	30.0000
−28.5	−0.0090	−0.0090	−0.0090
−18.0	−0.0090	−0.0090	−0.0090
−11.3	−0.0090	−0.0090	−0.0090
−06.5	−0.0345	−0.0345	−0.0310
−06.0	−0.0580	−0.0580	−0.0485
−04.0	−0.0567	−0.0567	−0.0470
00.0	−0.0385	−0.0385	−0.0350

accumulation was modeled to include a combination of benthic and pelagic sources. In the simulation, the resulting geometries were very sensitive to small changes in the accumulation rate with depth and time, so too much or too little progradation, respectively occurred with small increases or decreases in carbonate rate. Note that the accumulation rate fell rapidly in water deeper than 50 m (Table 7).

Pelagic deposition is a critical source of carbonate sediment and comes directly from the water column. In the simulation this pelagic 'rain' is defined as an accumulation, whose rate varied as a function of time (Table 8). This rate was used to provide sufficient basin fill across which the progradational basin margin built out as benthic carbonate.

3.10. Carbonate parameters

As in nature, the simulation limits the build up of carbonate to sea level. Excess carbonate accumu-

Table 7
Input parameter used during simulation of the Andros channel (see text for detail) — benthic carbonate deposition (BCD) rates

BCD rates (m/ka) at different depths as a function of times					
Depth (m)	Time in million years				
	−28.50	−17.00	−11.30	−03.00	00.00
−300	0.00	0.00	0.00	0.00	0.00
−200	0.07	0.07	0.07	0.04	0.07
−50	0.07	0.07	0.07	0.04	0.07
−15	0.35	0.35	0.35	0.04	0.35
00	0.40	0.40	0.40	0.04	0.40

Table 8
Input parameter used during simulation of the Andros channel (see text for detail) — pelagic carbonate deposition (PCD) rates

Variation of PCD rates (m/ka) across the basin as a function of time								
Time (Ma)	−28.50	−24.50	−11.50	−11.00	−4.50	−3.50	−2.50	0.00
Rate	0.0280	0.0217	0.0100	0.008	0.008	0.008	0.080	0.080

Table 9
Carbonate input parameters used during simulation of the Andros channel (see text for detail)

Talus/turbidite depositional angle (°)	20
Percent talus (%)	30
Percent turbidite (%)	70
Talus penetration distance (m)	1.0
Turbidite penetration distance (m)	10.0

lation is transported off the buildup and deposited seaward as talus and turbidites. The simulation algorithm assumes that all of the carbonate talus on the margin came from the 'reef' crest. The transported carbonate had an angle of repose that was 20°, with a distance of transport of 1 km for the apron of sediments and 10 km for turbidites (Table 9). The angle of repose of 20° was important for deposition of these mass gravity flows. Carbonates have a high angle of repose, which increases with cohesiveness (Kenter and Schlager, 1989). These values were set at the beginning of each simulation run. The percentage of the talus that was transported downslope off the carbonate platform into the basin was input as 20% of all the transported carbonate (Table 9).

3.11. Experiments with the simulation

Several experiments were performed in order to improve the match of the simulation to the seismic. Once the shape of the initial basin surface was determined, the elevation of that surface had to be positioned in such a way that, at the end of the simulation run, there was an exact fit of the sedimentary fill of each of the sequences to the accommodation. The shelf accommodation was tuned first and the offlapping clinoforms second. With a fixed sea-level curve as input, this match was dependent upon both subsidence rates and rates of carbonate accumulation. Ultimately, the subsidence rate was kept constant at 0.009 m/ka from 28.5 to 11 Ma through several sea-level cycles. Thereafter, the subsidence rate was increased to match the actual fill of sediments for that time interval.

Once subsidence was determined, the rate of benthic carbonate accumulation and that of pelagic deposition were established separately and coordinated with each other. Two sets of experiments were performed for this purpose. In one, over specific time intervals, the benthic carbonate rates were varied while the rate of pelagic accumulation was kept constant. In another, benthic carbonate rate was kept constant for a specific time interval (but varied at different time intervals) while the rate of pelagic accumulation was changed. In each case the resulting simulation was matched step by step with the seismic interpretation. In some cases, when it appeared that there was a lack of match between the simulation and the interpretation, the ages assigned to a sequence boundary were changed. For instance the sequence boundary first assigned an age of 17.5 Ma was changed to 25.5 Ma so the simulation geometries and the interpretation matched. Similarly, the sequence boundary assigned the age of 25.5 Ma was later changed to 24.7 Ma. For these changes in the interpretation it is assumed that the Neogene Curve (NC) is valid.

Additionally, erosional surfaces were created at the interpreted type I sequence boundaries of 11.3, 5.5 and 3.9 Ma. These erosional events are clearly displayed on the seismic and the 3.9 Ma boundary has a particularly irregular erosional surface. To simulate this erosion, deposition was simulated up to the time of erosion and paused. The upper surface of the simulation was then compared to the seismic interpretation and the excess sediment removed, so an unconformity was created that matched the seismic.

The experiments showed that a unique combination of the two sources of carbonate and a unique subsidence history produced the best match between the simulation and seismic. This combination of benthic and pelagic rates produced the matching dimensions of the prograding and aggrading sediment

wedges without oversteepening the prograding clinoforms. The timing and sequences of progradation were controlled by the size and timing of the sea-level excursions. Many iterative attempts were also made to develop similar geometries, with different sea-level curves and different values of the input parameters. While it was possible to produce similar prograding and aggrading geometries, it was not possible to match the output to the seismic interpretation. For example, Pomar (1993) suggested the use of series of sine curves to represent sea-level behavior in the Neogene. A few simulation runs were performed with sinuous sea-level curves of different wavelength and magnitude. While interesting results were achieved, the resulting simulations did not match the seismic.

3.12. Sequential results from the Bahamas simulation execution

When examined in detail, it is possible to see that all of the simulation-produced sequences match the seismic sequences. The illustrations in Figs. 4 and 5 track the geometry and timing of the evolving sedimentary fill of the Neogene of the Great Bahamas Bank as seen on the seismic and simulation, respectively. Tables 4–9 shows the variation of the different input parameters through the simulation time period.

4. Discussion and conclusions

The laterally stacked sequences of a seismic section are the product of tectonic movement and carbonate accumulation and also of sea-level changes whose signal can be identified by making sequence stratigraphic interpretations (Vail, 1988). As Eberli et al. (1994) indicated, a sedimentary simulation can successfully reproduce the geometries seen on a seismic line. The seismic data which document the sedimentary fill of the Straits of Andros exhibit a series of onlapping and downlapping wedges with various angles of slope. The simulation output produces a match with the seismic interpretation, and helped to quantify individual factors controlling aggradation and progradation in the Bahamas. It showed that different basin depths effected the timing and extent of progradation. It also showed that there was a close balance between aggradation and progradation, and that small changes in the rate of relative sea-level movement and/or carbonate accumulation rates caused immediate switches from aggradation to progradation in the margin. Progradation took place after the space that existed on the upper slope had been reduced and the sediment transported offbank was able to fill the remaining space downslope so extending the platform margin farther basinward. In particular, progradation was triggered by sea-level drops that shifted sediment production and accumulation to the margin slope. Carbonate production rates similar to modern rates were required to produce the sediment necessary for progradation, which suggests that carbonate production has been consistently high since the early Tertiary. At the same time repeated exposure and erosion have reduced the overall preservation and decreased the overall accumulation rate. Progradation occurred in pulses which are recorded on the seismic lines and are confirmed by the simulation to be a succession of prograding and sigmoidal sequences, with each sigmoid clinoform apparently having formed as a result of a single cycle of sea-level fall and rise (Eberli and Ginsburg, 1989). Each prograding sequence was up to 500 m thick and probably consisted of an offlapping complex of reefal carbonates covered by calcareous sand. Eberli and Ginsburg (1989) thought that during the transgressive stages, marginal reefs were established and then buried during the subsequent highstand, when abundant sediment was produced on the flooded bank. Their interpretation was based on findings from the leeside of the modern bank where early Holocene reefs are covered by offbank transported sand (Hine et al., 1981). The two 1990 core borings on the western margin of the Great Bahamas Bank have confirmed this interpretation. This interpretation justified the use of benthic accumulation, as well as a background pelagic rain, to produce the geometries during the simulation run. Interestingly, the simulation suggested progradation of the bank margin continued at sea-level lows even though the platform was exposed. It would appear that either in situ accumulation remained high at sea-level lows or that the platform sediments were eroded (which was not modeled in the study). For a carbonate shelf setting with a low rate of subsidence and a high rate of sedimentation, very clear stratigraphic signals

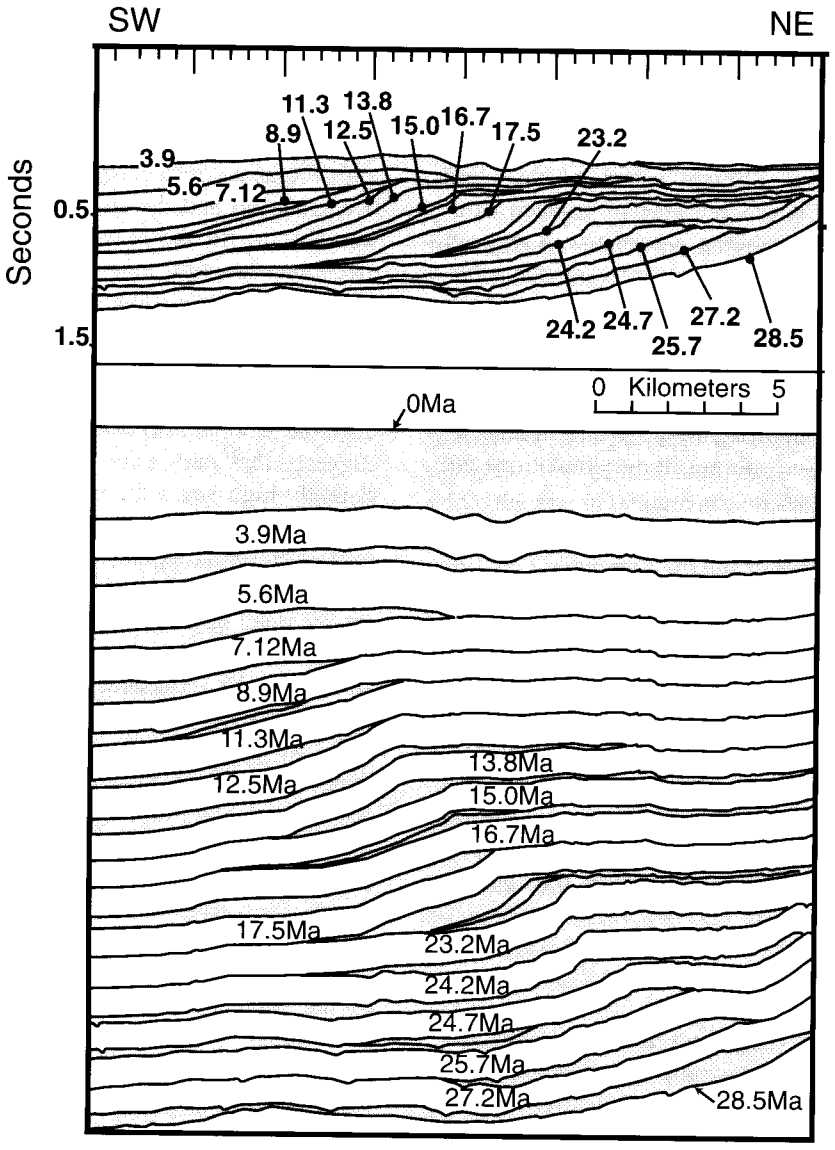

Fig. 4. The seismic section modeled, with individual interpreted sequences shown separately with ages for the sequence boundaries. Ages except for 28.5 Ma refer to top of sediment packages.

are produced by eustatic sea-level changes. This requires that the rate of carbonate sedimentation be such that the accommodation was filled to sea level, suggesting that the sediment surface on the shelf can be taken as a proxy of this sea level. For such a case, when (1) the rates of subsidence and carbonate accumulation were constant during several sea-level cycles, and (2) there was a match in the frequency and amplitude of the onlapping geometries of seismic and simulation, then it can be assumed that the frequency and amplitude of eustatic events of the input curve, the corrected Neogene curve used for this study, is close to reality. This match in the seismic and the simulation geometries established that eustatic sea-level charts can be used to date seismic sequence boundaries, as was the case of the Neogene carbonate platform of the of Straits of Andros in Bahamas. It also shows that computer simulations can

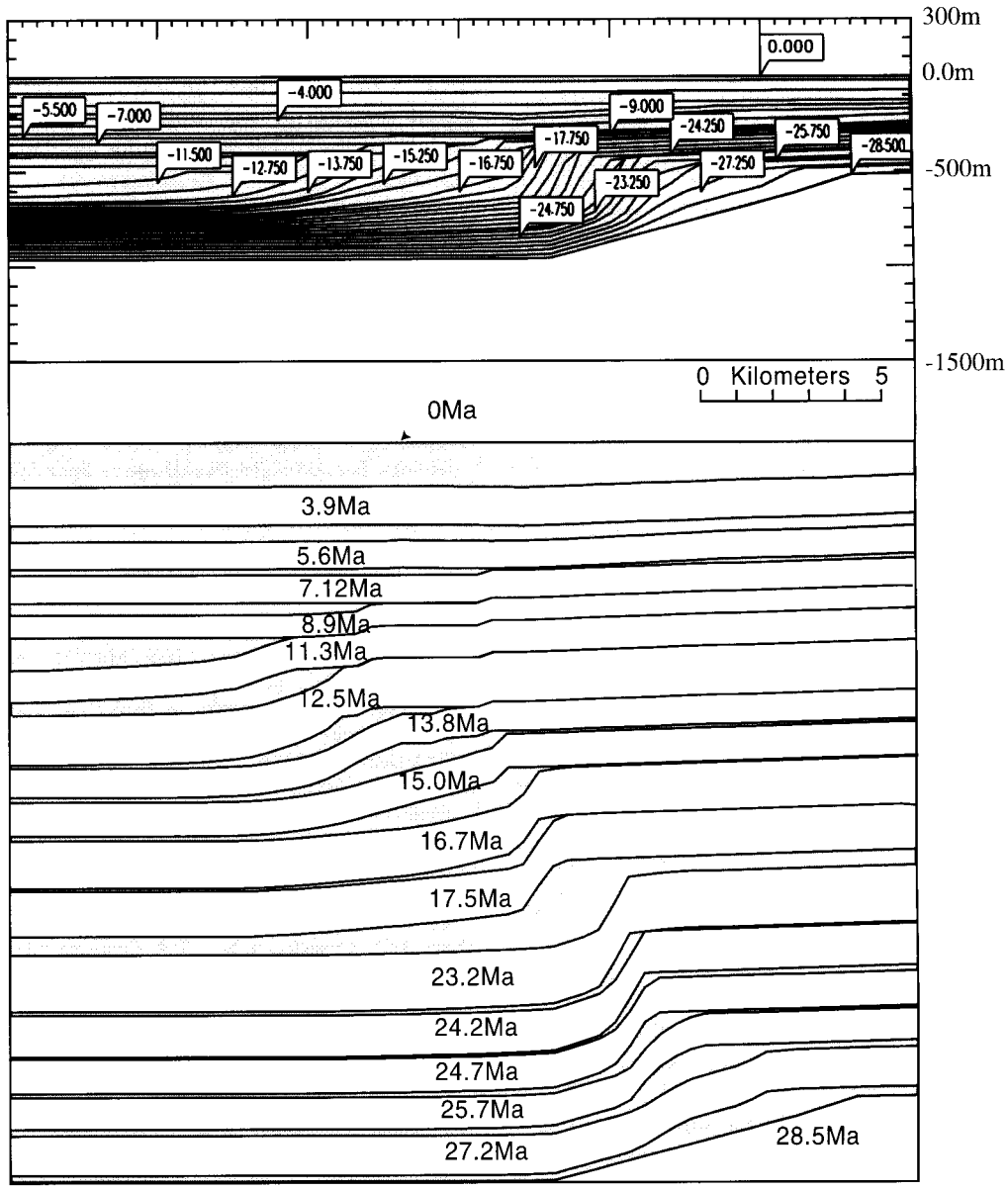

Fig. 5. Simulation output showing the modeled sequences separately along with the resultant sequence boundary ages. Ages except for 28.5 Ma refer to top of sediment packages.

be used to test seismic interpretations and update the ages of sequence boundaries when biostratigraphic data are poor.

When the result of the final simulation run was compared with results of ODP Leg 166 preliminary reports, a match for most of the sequence boundary ages was obtained but there were mismatches for a few ages (Table 10). The ages of the OPD SSBs are based on biomarker species horizons and the use of interpolated sedimentation rates between them. One might argue that the mismatch is because the Haq et al. (1987) chart is inaccurate or that some events are not as global as was thought. On the other hand the mismatch may be produced by a tectonic signal

Table 10
Comparison of the sequence boundary ages of ODP Leg 166 and the sequence boundary ages from the Neogene curve (NC)

ODP 166 SSB ages (Ma)	Cycles	Haq (updated) SSB ages (Ma)	Difference (Haq–ODP)
0.1			
0.6	TB 3.10	0.7	(+0.1)
1.7	TB 3.9	1.8	(+0.1)
	TB 3.8	2.3	
3.1	TB 3.7	3.1	0
	TB 3.6	4.3	
3.6	TB 3.5	3.9	(+0.3)
5.6	TB 3.4	6.1	(+0.5)
8.7	TB 3.3	7.2	(−1.5)
9.4	TB 3.2	9.1	(−0.3)
10.7			
	TB 3.1	11.3	
12.1			
12.7	TB 2.6	12.6	(−0.1)
	TB 2.5	13.8	
15.1	TB 2.4	15.4	(−0.3)
16	TB 2.3	16.4	(−0.4)
18.3	TB 2.2	17.3	(−1.0)
19.4	TB 2.1	20.6	(−1.2)
23.2	TB 1.5	21.6	(−1.6)
23.7	TB 1.4	24.5	(+0.8)
	TB 1.3	25.6	
	TB 1.2	27.1	
	TB 1.1	28.5	

Fourteen sequences of ODP Leg 166 were identified on the Neogene Curve (NC) and a comparison of their ages shows that nine have a difference of $\leq$0.5 Ma.

mixed with a global sea-level signal, producing leads and lags in the formation of sequence boundaries. However, the fact that the two age models, the one we developed here and the other from ODP, match so closely, is compelling.

The encouraging results of this simulation of a carbonate platform, suggest that simulations should be performed for other areas to see if dating of sedimentary sections can be achieved using sea-level charts and simulations. If this is successful then simulations may be used as tools for dating similar sections where biostratigraphy is poor.

Acknowledgements

We would like to acknowledge John Reistroffer and Parvita Siregar for their initial interpretations of the seismic cross-section. Dr. Dan Gill and Dr. Gregor Eberli are acknowledged for their critical reviews of the manuscript during preparation. The initial manuscript was immensely improved after critical review of Dr. Peter Sadler and Dr. Wolfgang Schlager.

References

Berggren, W.A., Kent, D.V., Swisher, C.C. III, Aubry, M.P., 1995. A revised Cenozoic geochronology and Chronostratigraphy. In: Berggren, W.A., Kent, D.V., Hardenbol, J. (Eds.), Geochronology, Time Scales and Global Stratigraphic Correlations: A Unified Temporal Framework for an Historical Geology. Soc. Econ. Paleontol. Mineral. Spec. Publ. 54, 129–212.

Bird, K.J., Molenaar, M.C., 1992. The North Slope Foreland Basin, Alaska. In: Macqueen, R.W., Leckie, D.A. (Eds.), Foreland Basins and Fold Belts. Am. Assoc. Pet. Geol. Mem. 55, 363–393.

Brown, L.F., Benson, J.M., Brink, G.J., Doherty, S., Jollands, A., Jungslager, E.H.A., Keenan, J.H.G., Muntingh, A., Van Wyk, N.J.S., 1995. Sequence Stratigraphy in Offshore South African Divergent Basins: An Atlas in Exploration for Cretaceous Lowstand traps by Soekor (pty) Ltd. Am. Assoc. Pet. Geol. Stud. Geol. 41, 184 pp.

Burton, R., Kendall, C.G.St.C., Lerche, I., 1988. Out of our depth: on the impossibility of fathoming eustasy from the stratigraphic record. Earth Sci. Rev. 24, 237–277.

Eberli, G.P., Ginsburg, R.N., 1987. Segmentation and coalescence of platforms, Tertiary, NW Great Bahama Bank. Geology 15, 75–79.

Eberli, G.P., Ginsburg, R.N., 1989. Cenozoic progradation of NW Great Bahama Bank — a record of lateral platform growth and sea level fluctuations. Soc. Econ. Paleontol. Mineral. Spec. Publ. 44, 339–355.

Eberli, G.P., Whittle, G.L., Kendall, C.G.St.C., Cannon, R.L., Moore, P.D., 1994. Testing a seismic interpretation of the great Bahama bank with a computer simulation. Am. Assoc. Pet. Geol. Bull. 78, 981–1004.

Eberli, G.P., Swart, P.K., Malone, M.J., et al. (Eds.), 1997. Shipboard Scientific Party, Site 1003. Proc. ODP Init. Rep. 166, 71–151.

Haq, B.U., Hardenbol, J., Vail, P.R., 1987. Chronology of fluctuating sea levels since the Triassic (250 million years ago to present). Science 235, 1156–1167.

Kendall, C.G.St.C., Strobel, J., Cannon, R., Bezdek, J.C., Biswas, G., 1989. The simulation of the sedimentary fill of basins. J. Geophys. Res. B, Solid Earth Planets 96(4), 6911–6929.

Hine, A.C., Wilber, R.J., Bane, J.M., Neumann, A.C., Lorenson, K.R., 1981. Offbank transport of carbonate sands along open, leeward bank margins: northern Bahamas. Mar. Geol. 42, 327–348.

Kenter, J.A.M., Schlager, W., 1989. Comparison of shear strength

in calcareous and siliciclastic marine sediments. Mar. Geol. 88, 145–152.

Miall, A.D., 1990. Principles of Sedimentary Basin Analysis. Springer, New York, NY, 668 pp.

Moore, P.D., 1997. Sedimentary Simulations: Design and Application of SEDPAK. Unpublished Ph.D. dissertation, University of South Carolina, Columbia, 95 pp.

Pomar, L., 1993. High-resolution sequence stratigraphy in prograding Miocene carbonates: Application to seismic interpretation. In: Loucks, R.G., Say, J.F.R. (Eds.), Carbonate Sequence Stratigraphy. Am. Assoc. Pet. Geol. Mem. 57, 389–407.

Ryan, S., 1997. Age determination from depositional sequences — analysis and stratigraphic simulation of the Lower Cretaceous Torok and Nanushuk Formations, North Slope of Alaska. Unpublished Master's thesis, University of South Carolina, Columbia, 63 pp.

Schlager, W., 1981. The paradox of drowned reefs and carbonate platforms. Geol. Soc. Am. Bull. 92, 197–211.

Strobel, J., Cannon, R., Kendall, C.G.St.C., Biswas, G., Bezdek, J.C., 1989. Interactive (SEDPAK) simulation of clastic and carbonate sediments in shelf to basin settings. Computers Geosci. 15(8), 1729–1290.

Vail, P.R., 1988. Seismic stratigraphy interpretation procedure. In: Bally, A.W. (Ed.), Atlas of Seismic Stratigraphy. Am. Assoc. Pet. Geol., Stud. Geol. 27, 1–10.

Vail, P.R., Mitchum, R.M. Jr., Todd, R.G., Widmier, J.M., Thompson, S. III, Sangree, J.B., Bubb, J.N., Hatlelid, W.G., 1977. Seismic stratigraphy and global changes of sea level. In: Payton, C.E. (Ed.), Seismic Stratigraphy — Applications to Hydrocarbon Exploration. Am. Assoc. Pet. Geol. Mem. 26, 49–212.

Wilber, R.J., Milliman, J.D., Halley, R.B., 1990. Accumulation of Holocene banktop sediment on the western margin of Great Bahama Bank: modern progradation of a carbonate megabank. Geology 18, 970–975.